Study On the Layout of Heliostat Mirror Field Based on Hybrid Strategy with Simulated Annealing Particle Swarm Optimisation Algorithm

Xinyu Zhao *

School of Mechanical and Energy Engineering, Tongji University, Shanghai, China, 201800

* Corresponding Author Email: 2153314@tongji.edu.cn

Abstract. Tower solar thermal power generation is a new type of green and environmentally friendly power generation technology. As the basic component for collecting solar energy, the position, angle and size of the heliostat are closely related to the power of the power station. In this paper, the mathematical physics method is used, and the improved particle swarm optimisation algorithm with simulated annealing process is adopted to derive the calculation model of output power per unit area and the optimisation scheme of the heliostat field.The innovation of this paper is to take into account the shading of incident and reflected rays at the same time to establish a comprehensive mathematical model; in addition, this paper also adopts the particle swarm optimisation algorithm to solve the layout problem of the heliostat field.Firstly, in order to calculate the optical efficiency and output power per unit area of the heliostat, this paper proposes a new shadowing loss model and a truncated efficiency loss model based on the combination of ray tracing method and planar projection method; secondly, the improved particle swarm optimization algorithm with simulated annealing process (SAPSO) is used to calculate the optical efficiency and output power per unit area of the heliostat, and the optimal solution for the independent variable is searched for the positional coordinates of the absorber tower, the size of the heliostat, the mounting height, the number of heliostats, and the location of the heliostat.

Keywords: Tower Solar Thermal Power, Photovoltaic Efficiency Loss Modelling, Heliostat, SAPSO.

1. Introduction

As the world's second largest economy, China's carbon emissions recently ranked first in the world, of which the power industry accounts for 40% of China's total carbon emissions [1]. In order to achieve the goal of "carbon peak - carbon neutral", China's power system has begun to green low-carbon transition, new energy [2] power generation is booming, tower solar thermal power generation as a green new clean energy technology has also made great progress. The heliostat is the basic component of the tower power station, with a horizontal axis that can control the pitch angle and a longitudinal axis that can control the azimuth angle, the heliostat reflects the sun's rays to the collector at the top of the absorber tower, and the collector converts the solar energy into heat and stores it, which is eventually converted into electrical energy. The position of the heliostat will directly affect the light path of the solar rays and thus the absorption efficiency of the collector, so the layout of the heliostat has attracted more and more attention.

For the layout problem of heliostat, Gao Bo [3] and others established the optical efficiency model of heliostat field of photothermal power station on the basis of the unobstructed (EB) layout model, and got the optimal layout scheme by using the improved whale optimization algorithm; Yang Hongtao [4] studied the whole process of the formation of the reflected spot from a single heliostat mirror, and selected the improved genetic algorithm for solving the periodic optimization mode, and selected BP Liu Jianxing [5] used MATLAB simulation technology to establish a mathematical model of the optical efficiency of the heliostat field, and used adaptive gravity search algorithm to find the optimal combination of row spacing until the annual average integrated efficiency of the mirror field reaches the maximum, and finally took the heliostat field of the Gemasolar tower-type photovoltaic power plant in Seville as an example to verify the method, proving that the method of the heliostat field is not a good choice for the solar field, but it is a good choice for the solar field. Finally, the

method is validated with the example of a fixed-sun mirror field at the Gemasolar tower solar power plant in Seville, which proves the feasibility of the method.

Scholars have conducted a large number of in-depth studies on the layout optimisation of the heliostat field, but most of them focus on the optimisation of a single variable (position, distance, etc.), and few studies have been conducted on the model of multi-variable integrated optimisation. Therefore, this paper makes use of the particle swarm algorithm with strong global search ability to carry out multi-factor co-optimisation, and at the same time combines the idea of simulated annealing to overcome the defects of PSO which is easy to fall into the local optimum and solves to obtain the optimal coordinates of the absorption tower position, size of heliostat, mounting height, number of heliostats, and position.

2. Optical efficiency modelling of heliostat fields

Data sources:

http://www.mcm.edu.cn/html_cn/node/c74d72127066f510a5723a94b5323a26.html

Includes sizing of heliostats and collectors, distribution range requirements, as well as formulas for calculating atmospheric transmittance and local elevation, latitude, longitude, and solar altitude.

2.1. Optical efficiency modelling

Firstly,the optical efficiency model of the heliostat fiel has been built in this paper, which consists of calculating the shadow shading loss, atmospheric transmittance, specular reflectance, cosine loss, and truncation efficiency [6]. The cosine loss is caused by the angular deviation between the sun and the mirror normal; the truncation efficiency is the efficiency of the heat absorber to absorb heat, which is the ratio of the radiant energy projected onto the heat absorber to the radiant energy reflected from the heliostat, and is related to factors such as collector dimensions, heliostat arrangement, and the orientation of the sun; atmospheric transmittance is the attenuation of the sunlight in the air propagation process due to the influence of dust, etc., which can be obtained according to the relevant formulas and physical location; specular reflectance can be identified as the shadow blocking loss, specular reflectivity, cosine loss, and truncation efficiency [6]. ; Mirror reflectivity can be identified as a constant; shadow blocking loss that is, the shadow side of a fixed-sun mirror to cover the mirror of another fixed-sun mirror, or reflected light to the back of another fixed-sun mirror or all other light-blocking substances on the mirror surface coverage. The following paper explains the calculation model of these kinds of efficiency in turn.

2.2. Description of the shadowing occlusion efficiency model

For the calculation of shadow shading efficiency, scholars at home and abroad have proposed a variety of calculation methods: for example, RCELL, MIEVAL, etc. Each of the above calculation methods has its own advantages and disadvantages. Each of the above calculation methods has its own advantages and disadvantages, and they can be divided into two kinds of calculation principles: ray tracing method and plane projection method. In this paper, a new calculation model based on these two principles is proposed.

Shadow shading mainly has the following three sources ① rear fixed-sun mirror in the incident sunlight part of the front fixed-sun mirror blocked by the shadow loss. ② rear row of solar mirrors in the reflection of sunlight is blocked by the front mirror and did not reach the collector of the blocking loss ③ tower on the mirror field caused by the shadow loss; based on the solar azimuth of the coordinate system transformation, due to the difference in the measurement of the moment, in order to simplify the calculation of the problem, this paper here is always set to the direction of projection of the sun's rays on the ground for the negative direction of the coordinate axis, i.e., each time the axis will be rotated in the positive direction of the sun's azimuth of the number of degrees.

As shown in Figure 1, this paper is based on the direction of solar incidence on the heliostat field for banded area division, x, y axis for the distribution range, it can be proved that due to the plane of

the sun's incident light is always perpendicular to the plane of the heliostat, the shadows on the ground in front of the heliostat in the ground always fall in the direction of the incident light in the shadow of the ground, the banded area for a reasonable division of a larger range of cases can be identified as the shading occurs in the division of the region.

As shown in Figure 2: W is the diagonal length of each mirror, i.e., the characteristic length, x is the straight line distance between the centres of adjacent mirrors; with the centre of the heliostat as the centre and the characteristic length as the radius of the circle, the tangent pattern can be made by extending the direction of sunlight incidence, and it is not difficult to prove that only in the red rectangle (2W× x) within the red rectangle (2W), it is not difficult to prove that only the heliostat within the red rectangle (2W× x) has the possibility of obscuring the target heliostat.

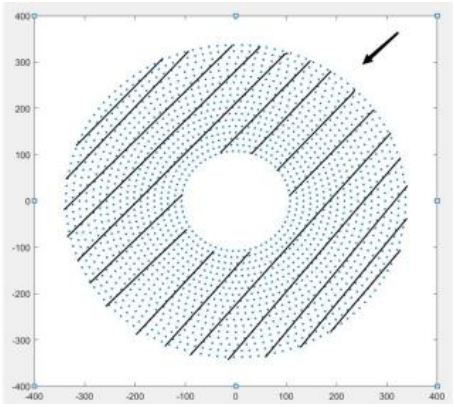


Figure 1. Schematic diagram of the zones according to the direction of solar incidence.

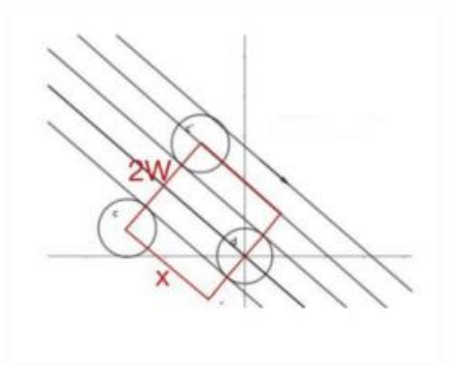


Figure 2. Areas that may be obscured

Planar projection calculation with the idea of light tracking: select the target heliostat A in the delineated strip area to study the obscured situation in turn, and determine the problematic heliostat B in the strip area that may cause shadow obscuration to mirror A. Here, as the position of the heliostat and the related parameters are determined, the calculation of the shadow obscuration situation can be realised, and the specific calculation method is given here:

Adopting the idea of ray tracing, set a sufficient number of dots on board B, according to the coordinate data in order to find its projection coordinates on the plane of board A. If the distribution is within the range of board A, it is considered to be shaded, and finally calculate the ratio of the number of dots in the range to the total number of dots.

However, due to such a point taking method only when the distribution of points is dense enough, to better respond to the shadow situation, and due to the region delineation method in this paper, the AB mirror away from the range is very limited, the two where the plane angle is basically approximate, which makes most of the shadow of the B-mirror can always be the A-mirror to achieve the whole piece of the coverage (schematic). Due to the symmetry of the field, in the distribution area ① case distribution can offset each other, and ② case very small area shadows on the overall calculation of the impact is very small, here this paper is omitted, and only calculate the shading between the AB mirror, the figure shows the simplest case, here due to the position of the fixed heliostat is given, the

sunlight and other parameters are given, you can directly calculate the shaded portion of the overall portion of the area of the overall portion of the area of the original point shown in Figure 3, the origin for the fixed heliostat As shown in Figure 3, the origin is the fixed point of the heliostat, and the mutual shading between the two rectangles simulates the mutual shading of the heliostat, and the shaded part is the projected area.

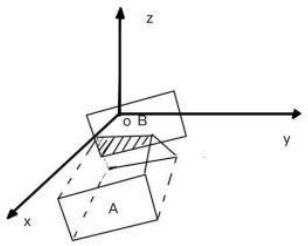


Figure 3. Schematic diagram of shadow masking loss

And even if the cases are not identical and the pitch angle of the plate changes, the shaded regions can still be treated as bands due to the similar position of the heliostats found by the method and the approximate parallelism of the plates, and the plane where the plate is located is perpendicular to the plane where the sunlight rays are located, and the computational errors caused by the irregular figure shapes are also cancelled out here. The solution is carried out sequentially for each of the divided regions to obtain all possible shading cases, and then the shadow shading loss is calculated.

Occlusion loss of reflected rays the calculation of reflected rays is similar to that of incident rays, but the differences lie mainly in the understanding of the areas where occlusion may occur and the changes in geometric relationships that occur during the calculation of shadows. The delineation of the region of possible occlusion of the reflected light still follows the principle of the direction of the light. As the question given in the case of the sun's rays through the centre of the mirror always shoot to the collector centre, this paper considers taking the radial band area division. Similar to the solution of incident light, because the method to find the heliostat position is similar and the plate is approximately parallel, and the plane where the plate is located is perpendicular to the plane where the sunlight rays are located, the shaded area can still be treated as a band.

2.3. Projective modelling of truncation efficiency

Since the light from the sun is actually a conical beam with a half-angle spread of 4.65 mrad, the reflected light is also a conical beam, and it is sufficient to consider the boundaries of the reflected region, which requires the consideration of two losses:

As this paper is set up so that the normal vector is in the position of the centre line and the angular bisector of the sun rays, at this time, the projected area in the collector is not the actual area but the projected area on the collector, and the boundary of the projection once exceeds the boundary of the collector there will be an overflow, which will make the truncation efficiency lower; as the reflected rays are conical light cones, the projection boundary is actually formed by the point source at the edge on the fixed-sun mirror Envelope, which will undoubtedly make the projection area larger, there may be overflow. The following paper specifically to calculate these two kinds of losses:

Let the normal vector of the mirror A (x, y, z) be n_1 (x, y, z) of the mirror, and the normal vector of the plane where the collector diameter is located is n_2 (x, y, 0), after arithmetic thus obtaining the cosine of the projecting plane and the projected plane. Make η_{trunc1} for the first part of the loss caused by the truncation efficiency reduction, combined with the projection theorem, this paper discusses the critical state, for the light just full of the collector cross-section, at this time, the critical cosine value of the area of the fixed-sun mirrors and collector area of the ratio of the cos β critical = 0.6428, as a segmentation boundary:

$$\eta_{trunc1} = \begin{cases} 1 & \cos\beta \geq \cos\beta_{\lim} \\ \frac{S_J}{S_M}\cos\beta & \cos\beta \leq \cos\beta_{\lim} \end{cases} \tag{1}$$

The average truncation efficiency due to escape into the atmosphere is then:

$$\overline{\eta_{trunc1}} = \frac{\sum_i^N \eta_{trunc1}}{N} \tag{2}$$

Losses due to non-parallel rays: using the data for the Earth-Sun distance and the Earth radius it is possible to derive an approximate cone angle: the maximum d_{HR} = 350m, yielding a maximum error distance of only 15cm, relative to the 7m× 8m of the collector cross-section scale, which is of course negligible. Therefore, this paper specifies $\eta_{trunc} = 1$.

In summary, the truncation efficiency is calculated as:

$$\overline{\eta_{trunc}} = \frac{\sum_i^N \eta_{trunc1}}{N} \tag{3}$$

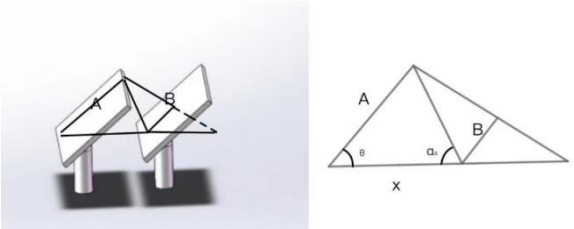


Figure 4. Schematic diagram of incident occlusion loss

As shown in Figure 4, this paper abstracts the graph on the left into a geometric relationship to obtain a geometric graph as shown on the right, whereθ is the angle made by the collector and the ground, αs is the sun's altitude angle, so that the height of the heliostat is 2l, and the distance of the neighbouring heliostat is x; at this time, the calculation of the incident shadow shading ratio λ_1 is not difficult to derive through the trigonometric relationship:

$$\lambda_1 = \frac{x\sin\theta}{2\sin(\alpha_s+\theta)\sqrt{l^2+x^2-2lx\cos\theta}} \tag{4}$$

Continuing with the calculation of the loss due to reflective occlusion, this paper defines λ_2 as the reflective shadow occlusion ratio λ_2:

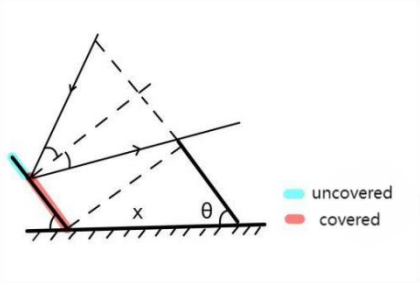


Figure 5. Schematic diagram of reflective masking losses

Again, after trigonometry, it's not hard to get:

$$\lambda_2 = \frac{x \sin\theta \tan(\alpha_s + \theta - \frac{\pi}{2})}{1 - \lambda_1} \tag{5}$$

From equation (2), it is easy to see that when the sum of the angle between the heliostat and the ground and the sun's altitude angle $\alpha_s + \theta$ is less than 90°, the formula is meaningless because the shading ratio cannot be negative, and at this time should be zeroed for all the λ2 that are less than zero. At this time, there is no reflective shading, as shown in Figure5, from η_{sb} = 1 - shadow shading loss, it's not hard to get:

$$\eta_{sb} = (1 - \lambda_1)(1 - \lambda_2) \tag{6}$$

The angle with the ground can be calculated from the normal vector of each fixed-sun mirror.θ The angle with the ground can be calculated from the normal vector of each fixed-sun mirror, and the angle with the ground can be found by substituting into the local αs at that time.λ_1 andλ_2 and then the shadow loss, and finally all the values are summed and averaged to get the average value.

The formula for the average cosine efficiency is η_{cos} = cosβ, βis the angle between the normal vector of the heliostat and the sunlight rays; the cosine value corresponding toβof each heliostat is averaged, and the average cosine efficiency can be obtained. By the coordinates of each heliostat and the vector of sun rays can determine the only normal vector (see above), in accordance with this normal vector in this paper can be obtained for each heliostat plane and collector projection surface of the cosine value, it is very clever, this paper is taken for the normal vector just for the centre of the line and the sun rays of the Angle Equidistant Line, so the cosine value of this paper can be used directly to cosine the efficiency of the η_{cos} On this basis continue to use MATLAB The stage efficiency of each heliostat can be solved and summed and averaged to finally get the average truncation efficiency.

2.4. Formula for calculating the annual power output of a fixed-sun mirror field

After solving the model in the previous section this paper has derived the average shadow shading efficiency η_{sb}, the average cosine efficiency η_{cos}, the average truncation efficiency η_{trunc} , and the formulae for the atmospheric transmittance have been given in the previous section:

Substituting into the formula:

$$\eta_{at} = 0.99321 - 0.0001176 d_{HR} + 1.97 \times 10^{-8} \times d \text{ HR2 } (d \text{ HR} \leq 1000) \tag{7}$$

Where d_{HR} is taken to be the distance from the midpoint of the heliostat to the centre of the heat absorber, and finally the average value is taken and substituted into Eq:

$$E_{field} = DNI \cdot \sum_i^N A_i \eta_i \tag{8}$$

The annual average output thermal power of the heliostat field can be obtained, in which the normal direct radiation irradiance DNI (unit: kW/m2) refers to the solar radiation energy received per unit area of the plane perpendicular to the sun's rays on the earth and per unit time, related to the local altitude and the sun's altitude, and it is a constant. i is the product of the optical efficiencies of the ith mirror, A_i is the area of the heliostat, and N is the number of heliostats;η_i is the product of the optical efficiency of the ith mirror. A_i is the area of the solar fixed mirror; N is the number of solar fixed mirror.

3. Optimising the layout of a fixed-sun mirror field using SAPSO

3.1. Problem domain description

Due to production specifications and site constraints, the heliostats are distributed in a concentric ring with a radius of 100m to 350m, with a mirror side length of 2m to 8m, an installation height of

2m to 6m, a mounting height of more than half the length of the mirror side, and a distance of 5m or more between the centres of neighbouring heliostat bases compared to the width of the mirrors. After obtaining the formula for calculating the annual output power, the parameters of the heliostat field (including the positional coordinates of the absorber tower, the size of the heliostat mirrors, the mounting height, and the number and position of the heliostat mirrors) are used to make the annual average output thermal power of the heliostat field per unit of mirror surface area as large as possible.

Thus, the problem domain can be described as a multivariate nonlinear optimisation problem:

$$Objecitve: Max(\frac{E_{field}}{\sum_i^N A_i})$$
$$Subjectto: 2 \leq \mathrm{L} \leq 8$$
$$1 \leq \mathrm{h} \leq 2$$
$$\mathrm{L} + 3 \leq \mathrm{x}$$
$$100 \leq \sqrt{\mathrm{x}^2 + \mathrm{y}^2} \leq 350$$

3.2. Particle swarm optimisation algorithm based on simulated annealing

Particle Swarm Optimization (PSO) [7] is an optimisation algorithm based on group intelligence, which finds the optimal solution by simulating the movement of individuals in the group in the search space. Simulated Annealing (SA) [8] is a stochastic search algorithm that simulates the physical annealing process, which accepts inferior solutions with a certain probability in order to jump out of the local optimal solution, so as to search for the optimal solution in the global range. It utilises information exchange and learning between individuals to improve convergence speed and accuracy. Simulated Annealing Particle Swarm Optimization (SAPSO) is a hybrid algorithm that combines the SA algorithm with the PSO algorithm, which uses the temperature parameter and the Metropolis criterion in the SA algorithm to improve the global optimal selection and speed update strategies in the PSO algorithm, so as to improve the PSO algorithm. It uses the temperature parameter and Metropolis criterion in the SA algorithm to improve the global optimal selection and speed updating strategies in the PSO algorithm to improve the performance of PSO algorithm.

The basic idea of the SAPSO algorithm is to introduce a temperature parameter into the PSO algorithm and gradually reduce the temperature according to an annealing function. This paper uses a roulette strategy to determine an alternative to the global optimum at each temperature and calculate its acceptance probability according to the Metropolis criterion [9]. If the alternative value is better than the current global optimum, it is accepted directly; if the alternative value is worse than the current global optimum, it is accepted with a certain probability. Then the velocity and position of the particle are updated according to the PSO algorithm, and a velocity compression factor is introduced to control the velocity range of the particle.

3.3. Solution steps

The solution steps of SAPSO are as follows:

1. Initialisation parameters and particle swarm. Set the parameters such as the number of particles N, the learning factors c_1 and c_2, the annealing constant lamda, the maximum number of iterations M, the number of independent variables D, the initial temperature T_0, etc., and randomly generate the positions and velocities of the N particles. The number of independent variables is the total number of heliographs.

2. Calculate the fitness value of the swarm. For each particle, calculate its objective function value as its fitness value, and take its current position as its historical optimal position. Then find the particle with the smallest fitness value among all particles and take its historical optimal position as the global optimal position. Here, the particle position in the original SAPSO algorithm is increased by one dimension, so that the particle position and velocity in the new algorithm become two-dimensional variables, and the coordinates of each helioscope are handled in this way.

3. Set the current temperature as the initial temperature, i.e. $T=T_0$.

4. Repeat the following steps until the termination condition is met or the maximum number of iterations is reached:

1) Calculate the global optimal fitness value, which is used to calculate the probability in the subsequent simulated annealing process.

2) Calculate the fitness value of each particle at the current temperature and use it to select the global optimal alternative value in the subsequent roulette strategy. According to the Metropolis criterion, the fitness value is inversely proportional to the fitness value, the worse the solution is, the more likely it will be accepted, in order to increase the diversity and exploration ability, this paper adopts the roulette strategy to determine the global optimal alternative, i.e., randomly select a particle among all particles according to the probability distribution as the global optimal alternative. This can increase the diversity and exploration ability and avoid falling into the local optimal solution. The particle adaptation value represents the probability of the (i)th particle at the current temperature, where (T) is the current temperature. The global optimal alternative pg_plus = x_k, where (k) is the first integer that satisfies the condition that the cumulative probability distribution function (CDF) is greater than or equal to the first index of the random number.

3) Normalise the adaptation values of each particle so that the sum of the adaptation values of all the particles is 1, obtaining a probability distribution. The normalised particle adaptation value represents the normalised probability of the (i) particle at the current temperature:

$$TF\ (pi)\ = \frac{e^{\frac{[f(pi)-f(pg)]}{t}}}{\sum_{i=1}^{N} e^{-\frac{[f(pi)-f(pg)]}{t}}} \tag{9}$$

4) Generate a random number in the interval [0,1] to be used in a roulette strategy to select the globally optimal alternative.

5) Calculate the sum of the learning factors for the subsequent calculation of the speed compression factor.

6) Calculate the velocity compression factor, which is used to control the velocity range of the particles to avoid too large or too small velocities, which may affect the convergence and stability.

7) Perform update operations for each particle, including velocity update, position update, fitness value update, historical optimal position update and global optimal position update. Update the velocity of the particle according to the formula of PSO algorithm and introduce random number and velocity compression factor to increase the randomness and convergence. Update the position of the particle according to the formula of the PSO algorithm, i.e., add the velocity value to the current position. If the fitness value of the particle's new position is smaller than the fitness value of its historical optimal position, then the particle's historical optimal position is updated as the new position. If the fitness value of the particle's historical optimal position is smaller than the fitness value of the global optimal position, then update the global optimal position to the particle's historical optimal position.

$$v_{i,j}(t+1) = \varphi\{v_{i,j}(t) + c_1 r_1[p_{i,j} - x_{i,j}(t)] + c_2 r_2[p_{g,j} - x_{i,j}(t)]\}$$
$$x_{i,j}(t+1) = x_{i,j}(t) + v_{i,j}(t+1) \tag{10}$$

8)Reducing the temperature by multiplying it by an annealing constant, lamda (0<lamda<1), results in a gradual decrease in temperature with the number of iterations, thus increasing convergence and stability.

9)Outputs the global optimal position as the value of the independent variable when the objective function takes the minimum value, and the corresponding objective function value as the minimum value of the objective function.

However, the above arrangement occurs for a given number of mirrors, and in fact In fact, it's hard to confirm whether it’s feasible to find a solution that uses fewer mirrors to make the optical efficiency of a single lens higher, this paper presents an SA search on the number of mirrors in the borrowed dataset, and two layers of SAPSO algorithms are nested in the SA algorithm, the first one is used to

search for the most suitable arrangement; the second one is used to calculate the optimisation of parameters of the mirror field under this layout mode, i.e., the size of the fixation mirror, the mounting height, and the mounting height. The second layer is used to calculate the optimisation of the parameters of the mirror field under this layout pattern, i.e., the size of the fixed-sun mirrors and the mounting height.

At the same time in the design process of the above algorithm to take into account the impact of constraints, here the hybrid penalty function method is used: this method is a combination of the outer-point penalty function method and the inner-point penalty function method [10], for the equation constraints to use the outer-point penalty function method, for the inequality constraints to use the inner-point penalty function method, so as to overcome the shortcomings of their respective defects. This method is suitable for the case where the constraints are a mixture of equations and inequalities, and also for the case where the initial points are outside or inside the feasible domain.

3.4. Results

After the parameter initialisation, the initial values of the number of fixed-sun mirrors, height, position coordinates, learning factor, etc. are set, the objective function is set to function [average]= fitness(x,y), the position vector is set as the incoming parameter, and the outgoing parameter is i.e., the final annual average output thermal power average.The optical efficiency and the output thermal power of each mirror are still calculated by the coordinates of each mirror using the optical efficiency and the output thermal power calculation method described in the above paper. The optical efficiency and annual average output thermal power of each mirror are calculated by coordinates. By constantly changing the range of changes in coordinates, such as the size of the circle changes, the circle is changed to a square area [11], etc., iterative testing of the maximum value of the output thermal power, at this time the distribution of heliostat mirrors, as shown in the Figure 6, approximate to the circle, the annual average optical efficiency is close to 57.832%.

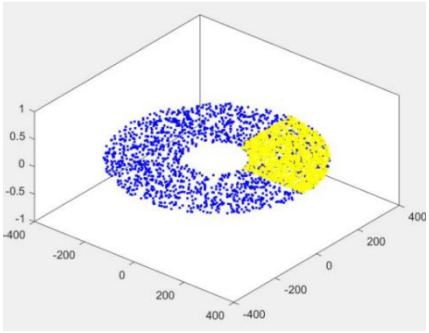


Figure 6. Spatial distribution of the heliostat field

Then the number of heliostats is varied, and the SA algorithm is used for search and find. Finally, the size and height of the heliostats are then varied. To reduce the model complexity, the dimensions are simplified to an integer from 2m to 8m for iteration. The final output is shown in Table 1.

Table 1. Optical efficiency of the optimised heliostat field and thermal power output per unit area

Average annual optical efficiency	Average annual cosine efficiency	Shadow Occlusion Efficiency	Annual cut-off efficiency	Annual thermal power output per unit area (mW/m2)
0.5252	**0.7179**	**0.8482**	**0.9138**	**2.0316**

4. Conclusions

In this paper, the optical efficiency model of heliostat field is constructed under the consideration of various factors such as occlusion, reflection, and scattering loss, and the optimal layout of heliostat with annual thermal power per unit area and average optical efficiency are derived using the model combined with the example swarm optimisation algorithm. The model algorithm in this paper can be

used to guide the layout of the heliostat field, thus saving cost and improving the utilisation of optical energy.

The actual heliostat field layout problem may be affected by other factors such as the area of the heliostat, the shape of the heliostat is not uniform and the rotation angle of the heliostat is limited, but this paper on the above factors are simplified to a certain extent, so the follow-up will also be the unequal area of the heliostat field problem will be discussed, and at the same time optimise the algorithms, to achieve the effect that the smaller computational power can be achieved as soon as possible to converge.

References

[1] SUN Jingyang,KONG Xiangyu,CHEN Yi,et al. An overview of carbon emission accounting methods for the whole link of power system[J/OL]. Power System Automation:1-14[2024-04-17].

[2] ZHOU Qixing,WANG Hui,OUYANG Shaohu. The construction of beautiful China based on new carbon neutral technology[J]. China Environmental Science,2024,44(04):1777-1787

[3] GAO Bo,SUN Hao,LIU Sheng. Optimal arrangement of mirror field in solar thermal power station based on improved whale algorithm[J]. Journal of Solar Energy,2023,44(10):209-217

[4] Yang Hongtao. Research on the model and optimal scheduling system of heliostat concentrator[D]. Xi'an University of Technology,2024

[5] Liu Jianxing. Optical efficiency modelling simulation and optimal arrangement of heliostat mirror field for tower-type photovoltaic power plant[D]. Lanzhou Jiaotong University,2023

[6] SUN Li-Peng,CHEN Bin-Hao,SHU Jian-Hao,et al. Computational model for the optical efficiency of a fixed-sun mirror field[J]. Mathematical Modelling and its Applications,2024,13(01):61-66

[7] Li Yanxia,Zhang Yanfang. Research on the optimisation of Internet of Things data mining check-all based on improved PSO particle swarm and K-Means clustering algorithm[J]. Yangtze River Information and Communication,2024,37(01):155-157

[8] LU Sheng-Feng. Computer simulated annealing optimisation algorithm monitoring model and simulation test[J]. Technology and Market,2024,31(03):87-91.

[9] LU Yanhong,YANG Feng,ZHAO Zichen,et al. Incomplete annealing-based forbidden search algorithm for normal clouds and applications[J/OL]. Microelectronics and Computers,1-13[2024-04-20].

[10] ZHANG Shouye,YANG Jingang. Introduction to several algorithms and mathematical experiments of common constrained optimisation problems[J]. Journal of Chifeng College (Natural Science Edition),2010,26(01):8-10

[11] Carrizosa E, Domínguez-Bravo C, Fernández-Cara E , et al.An optimisation tool to design the field of a solar power tower plant allowing heliostats of different sizes[J].International Journal of Energy Research,2017,41(8):1096-1107.